JET–P(99)54

O N Jarvis et al

Measurements of Escaping Fast Particles, using a Thin Foil Charge Collector

JET–P(99)54

Measurements of Escaping Fast Particles, using a Thin Foil Charge Collector

O N Jarvis, P van Belle, M Hone, G Sadler, G A H Whitfield,
F E Cecil[1], D Darrow[2], B Esposito[3].

JET Joint Undertaking, Abingdon, Oxfordshire, OX14 3EA,
[1]Colorado School of Mines, Golden, Colorado 80401, USA.
[2]Princeton Plasma Physics Laboratory, Princeton, New Jersey 08540, USA.
[3]Associazione Euratoe-ENEA sulla Fusione, C.P. 65, I-00044 Frascati (Rome), Italy.

Preprint of a Paper to be submitted for publication in Fusion Technology

January 2000

ABSTRACT

Two screened, thin foil, charge collectors were mounted just beyond the plasma edge at an outboard position (below mid-plane) in the Joint European Torus, to detect lost alpha-particles during the 1997 high fusion power D-T experiments. No convincing observations of alpha-particle collection were obtained, possibly due to the low level of alpha-particle losses, but more probably because the positioning of the detector was not ideal for the high fusion power discharges which were run at high plasma current and toroidal field. Under such conditions, alpha-particles on escaping orbits leading towards the detector are highly likely to be intercepted by the nearby poloidal limiter. Moreover, a small alpha-particle signal would have been obscured by interference from a large and unexpected signal attributed here to fast neutrals leaving the plasma and ionizing in the low density scrape-off region outside the plasma boundary. The interpretation of this unexpected signal is the subject of the present paper. In all probability, it will also be encountered in any future attempts to detect lost alpha-particles in a current measuring detector unless suitable precautions are taken, e.g. provision of a thin first foil to remove light charged particles with energies below about 0.5 MeV energy.

I. INTRODUCTION

The measurement of the losses of energetic alpha-particles to the vacuum vessel walls during high fusion power tokamak operation is of considerable interest [1], firstly, because any such losses would indicate inefficient heating of the plasma and, secondly, because the local power loading on plasma-facing components could result in serious damage and might therefore constitute a threat to the viability of the reactor concept.

A number of types of lost alpha-particle detector have been proposed and some have been tested [2], the simplest of which is based on the familiar Faraday cup charge collector used in most charged-particle accelerator facilities [3]. A constraint that has to be respected in the design of lost-alpha particle detectors for JET is the operation of the machine with its vacuum vessel walls raised to above 300 ^{o}C, so that use of scintillators (with their temperature sensitive responses) is impractical. Also, there are real problems of access and the time permitted for installation was severely restricted. Foreseeing such difficulties led to a simple detector based on the collection of charge being developed. Due to the large acceptance solid angle required to obtain a useful signal, orbit selection could be used only for a limited measure of energy resolution. Thus, in one of the two detectors a multiple thin foil arrangement was employed to provide a measure of energy discrimination by virtue of alpha-particle range in nickel. The desired signals are measured by sensing the current passing from each foil to ground.

The two detectors are located in the machine in the outer lower quadrant of the vacuum vessel, at about 0.4 m below the machine median plane and with their facing surfaces 0.105 m from the boundary surface containing the outer poloidal plasma limiters. The upper detector contains two nickel foils, each 250 μm thick, while the lower one (illustrated schematically in Fig. 1) contains

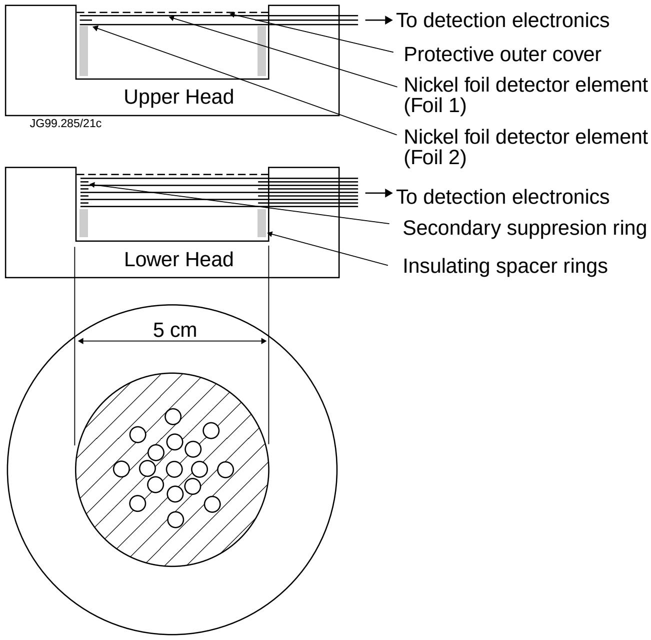

Fig. 1. Showing the construction of the two multi-foil detector assemblies, with the plan view for the lower assembly showing the 16 holes through the protective mask.

5 foils, each 2.5 μm thick. For D-T fusion-produced alpha particles with a mean energy of 3.5 MeV, the range in nickel is 5 to 6 μm. For the upper detector, all alpha-particles should stop in the first foil. For the lower detector, the alpha-particle produced current should appear principally in the second and third foils, for normal incidence. However, because the plane containing the foils was placed parallel to the magnetic field lines (to prevent δ-rays crossing from one foil to another), the alpha-particles are expected to enter with inclined orbits (less than 45^o to the foil surface) so few full-energy alpha-particles would be likely to pass through the first foil and into the second and none should reach the third. In both detectors, the rear foils provide a measurement of the noise in the signals due to sources other than alpha-particles.

Both detectors consist of foils 50 mm in diameter separated by 1.5 mm gaps, as indicated in Fig. 1. There is a mask in front of each set of foils that limits the active region to 0.92 cm^2 in the case of the upper detector and 3.70 cm^2 in the case of the lower detector. These masks were provided to limit the alpha-particle power deposited in the foils to a level below that which would melt the foils, with the smaller holes destined for the lower detector; however, the masks were inadvertently fitted as specified above. The detectors face the vessel walls, rather than the plasma, in order to avoid the possibility of energetic neutral particles striking the detector foils (although these should not give rise to any current) and to eliminate the possibility of photoelectron emission from soft X-rays. The soft X-ray flux in JET is such that if the detectors faced the plasma, the photo-emission current would (in the absence of the magnetic field) far exceed the expected alpha-particle current. In order to protect the detectors from excessive heating from the plasma, they are located with the plasma-facing surfaces about 5 cm in the shadow of the poloidal limiter. Despite the adverse geometry, the effect of the alpha-particle's grad-B and curvature drifts and gyromotion make it possible for alpha-particles to enter the detector (at least, for low values of toroidal field and plasma current).

Each foil is electrically insulated from all other foils and is connected by a superscreened cable to the detection electronics in the JET Diagnostic Hall outside the biological shield. The cable run is about 100 m long. The detection electronics for each channel consists of a sensitive current-to-voltage amplifier with a gain of 4.7×10^6 V/A with a 20 Hz low pass filter incorporated into it to reduce the noise. A follow-on isolation amplifier provides an additional gain of 10 and a 50 Hz low pass filter. Overall, the maximum output of 10 volts corresponds to 200 nA of collected current. The signals are digitized and recorded by the JET computer system.

The positions for the detectors (lower outboard quadrant) were selected after a study in which a random selection of alpha-particle birth points in the machine, tracked with a full-orbit code, showed that any loss to the walls is likely to be confined to the lower outer quadrant of the machine, including the divertor region (to which access is impractical). Unfortunately for the present purpose, the poloidal limiters distributed around the vessel will intercept most of the energetic charged particles before they reach the location of the detectors. Only those charged particles on extreme orbits have a reasonable chance of reaching the detector entrance aperture without being lost to the nearest upstream limiter. The orbits identified as having the highest likelihood of striking the detector are those originating at a minor radius in excess of r/a=0.5, on trapped orbits very close to the trapped-passing boundary. Particles on the outer branches of these orbits (travelling parallel to the plasma current), if they do not reach the detector, are all lost to the walls or limiters. The detection efficiency (alpha-particles detected per source alpha-particle) is computed to vary strongly with plasma current (I_p), toroidal field (B_T) and alpha-particle source radial profile; numerically computed values range from 10^{-7} for I_p=0.9 MA and B_T=0.9 T down to 10^{-14} for I_p=3.2 MA and B_T=3.5 T (Fig. 2).

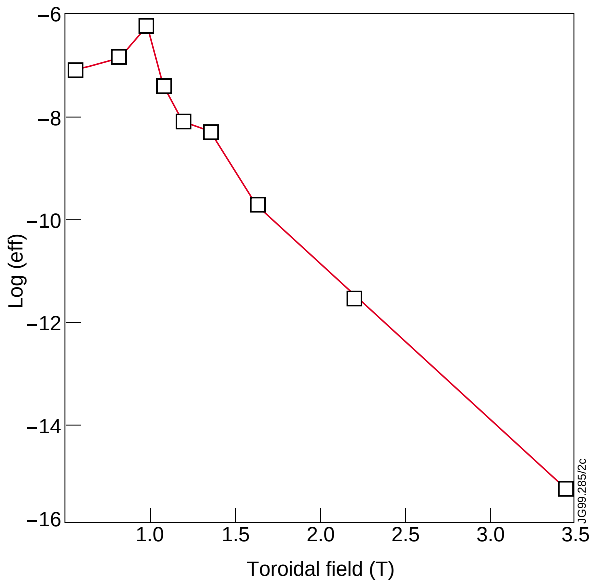

Fig. 2. Calculated efficiency for alpha-particle detection.

Measurable alpha-particle signals were expected for low field discharges where the alpha-particles are relatively weakly confined and limiter scrape-off should be least important. For example, the peak efficiency of 10^{-6} is associated with 1.0 MA, 1 T discharges, for which a modest peak fusion power of about 0.1 MW would give rise to a current of 12 nA. The best fusion performance, 16.1 MW, was achieved for a 4.0 MA / 3.6 T discharge, but under these conditions the detector efficiency is vanishingly small. The primary objective of this experiment was to study the effects of MHD disturbances, such as sawteeth, when the instantaneous losses can be orders of magnitude greater [4] than the quiescent loss rate. In the event, it is believed that the high performance discharges did not exhibit sufficiently strong MHD effects to have led to significant expulsion of alpha-particles from the plasma.

The best conditions for detecting the steady-state alpha-particle loss require the discharge to have a very broad neutron (alpha-particle) emission profile, typically encountered by applying high power beam heating to a high density target plasma with low plasma current and toroidal field. Regrettably, the diagnostic was not commissioned during the short period of time during the JET DTE1 experiment [5] when discharges of this type were being produced. Nevertheless, a number of discharges were run for which the alpha-particle loss signal should have been detectable had it not been for an even larger superimposed signal of unexpected origin, as will be described below.

The sensitivity of a future diagnostic for detection of alpha-particles could be greatly increased by placing it closer to the last closed flux surface than the present 105 mm distance to the outboard face, which is grossly excessive. This spacing was determined by the requirement that the plasma-facing surface be outside the plasma scrape off region, to minimize the power loading on the protective graphite tile, and to protect the thin foils, which are fragile and easily melted. Indeed, the front foil in a prototype detector tested prior to the DTE1 experiment did rupture during machine operations. The very compact, more robust and less heat sensitive design recently developed by Cecil [ref. 6] should be suitable for positioning appreciably closer to the plasma.

II. EXPERIMENTAL RESULTS

Despite the considerable care taken to provide screening against electromagnetic pickup between the detector heads and the signal conditioning equipment in the Diagnostic Hall, the signals were found to be quite noisy. Not all of this noise was associated with transmission from within the tokamak but was a feature of the general electrical environment. Under certain circumstances e/m pickup signals were recorded by all foils, in both detectors; these signals were associated with changing currents in poloidal field coils. The possibility that signals may be produced in the foils due to ICRH pick-up was also investigated, but no correlation was found with any of the four ICRH power modules.

In both detectors, only the first foils recorded genuine (i.e. other than noise) signals. The signals from the first foil in the upper detector were smaller by a factor of about 4 than those from the corresponding foil in the lower detector (and not larger by this factor, as they would have been had the masks been installed correctly). Subtraction of the second or third foil signals from the first foil signal for the 5-foil detector removed most of the pickup, leaving what we now believe to be a particle current ($I_{1st\ foil}$). The resulting noise level was of the order of 1 nA. Subtraction of the third foil signal from the second foil signal gave a difference that was residual noise only ($I_{2nd\ foil}$). Sometimes the difference signals showed oscillatory e/m pick-up from the plasma (correlated with the D_α signal), but in this case the time average of the signals from each foil was zero.

The data reported in this paper were obtained over the course of two successive experimental campaigns. The first data-taking period commenced after the initial low-power discharges of the DTE1 campaign had been completed but covered all the high power discharges and the subsequent clean-up period during which most of the tritium was exhausted from the vacuum vessel. The MkIIA divertor configuration was used for the DTE1 experiment. The interpretation of the measurements obtained with the thin-foil detector during this period form the bulk of this paper. After the DTE1 experiment had been concluded, the divertor geometry was changed to that of the MkIIGB (Gas Box) configuration. With the new divertor arrangement, it was found that the character of the measurements obtained with the thin-foil detectors was very different from the earlier experience. The interpretation offered here accounts for this altered situation.

III. RESULTS FROM THE DTE1 CAMPAIGN

A. Observations

The first period of study includes discharges in the DTE1 campaign (range 41949-44414) when the MkIIA divertor was in operation. The signal recorded for the 1 MA /1 T discharge number 42757 (Fig.3) reached 100 nA, somewhat larger than the 30 nA predicted for the alpha-particle current but nevertheless strongly suggestive of alpha-particle detection. More generally, for low plasma currents and toroidal fields - and in the absence of giant ELMs - the e/m-pickup-subtracted signal on the first foil was typically of order 10 nA to 100 nA in magnitude and was usually a reasonably faithful reproduction of the global neutron emission intensity, reducing in magnitude with increasing current/field. This was, at first, taken to be very encouraging but examination of data from subsequent discharges run with higher plasma current and toroidal fields demonstrated unequivocally that this difference signal was *not* always related to neutron emission. It is obvious that an additional signal of unexpected origin contributes strongly. Nevertheless, it remains the case that we cannot discount the possibility of an alpha-particle contribution in discharges such as that shown in Fig.3.

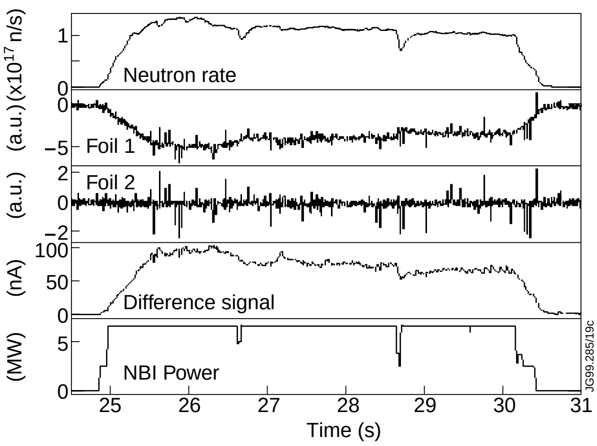

Fig. 3. Discharge 42757 with low plasma current and low toroidal magnetic field (I_p = 1 MA, B_T = 1 T). There is a modest d-t neutron yield (top) due to 7 MW - (3 MW 80 keV deuterium plus 4 MW 150 keV tritium) - of neutral beam heating (bottom). Foil 1 displays a very strong signal with some superimposed noise. The other foils show only noise. Subtracting foil 2 from foil 1, multiplying by -20, to obtain positive current results in the difference signal, which reaches $I_{1st\,foil}$ =100 nA.

We have found that the temporal dependence of the first-foil current is strongly correlated with the D_α-signal, with giant ELMs constituting the most prominent feature (Figs.4a and 4b). The initial sharp spike in the D_α-signal for each giant ELM is not mirrored by the detector signal, although the current rises afterwards towards a maximum and a subsequently decays in a manner that follow quite closely the base-level of the D_α-signal. In particular, the maximum in

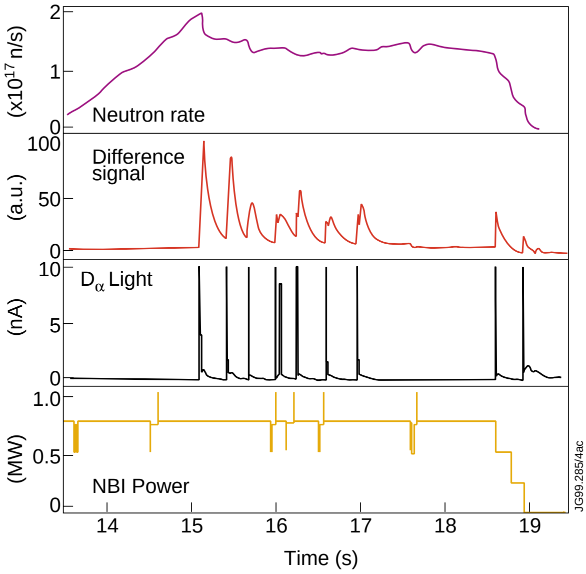

Fig. 4a. Discharge 42991: a 3 MA, 3 T discharge heated with 8 MW of tritium neutral beams. The figure illustrates the response of the detector to the D_α signal. The response to the giant ELMs is shown more clearly in Fig. 4b.

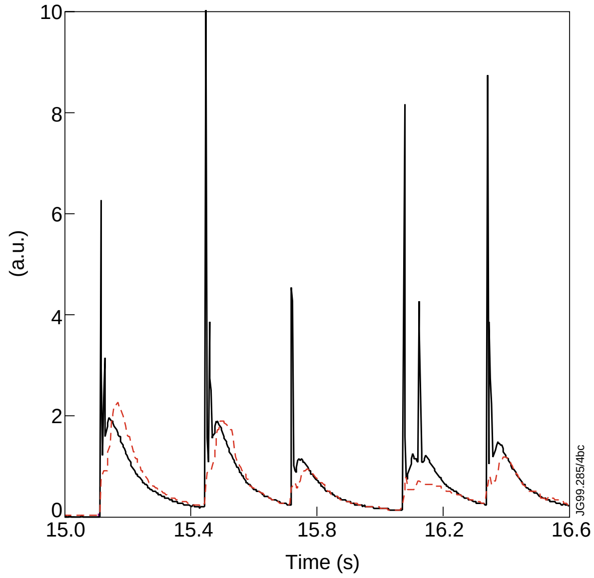

Fig. 4b. Discharge 42991: an overlay to display the way the D_α (solid line) fast spike is ignored but the slow decay is mirrored closely by the detector current (dashed line).

the detector signal lags about 40 ms behind the initial spike of the ELM. This is consistent with the idea [7] that an outer shell of plasma is lost into the divertor as a result of the instability causing the ELM, with generation of much light outside the plasma boundary. The plasma rapidly (in about 10 ms) expands to fill the original bounding surface, which is bombarded with a strong recycling neutral influx until equilibrium is restored. The super-thermal ions will have been lost from the affected plasma layer (perhaps 10 cm thick) and the 40 ms delay presumably represents the time taken to restore the fast ion population. (e.g. due to the slowing down of 160 keV beam ions). Sawteeth have not been observed to produce noticeable enhancements of the signal. As already stated, no obvious MHD-related alpha-particle losses have been identified.

B. Discussion

The second foil signal, which would have been strongly indicative of escaping alpha-particles, was never significantly above its noise level. This should not be taken as proof of the non-observance of alpha-particles because the angle of incidence at the detector foils (associated with the low detection efficiency) was such that penetration of the first foil may not have been possible.

The first foil signal, attributed here to relatively low energy (i.e. ~ tens of keV) ions, is not, despite appearances and initial expectations, uniquely and directly related to the emission of 14 MeV neutrons. This is unambiguously demonstrated in Fig. 5 by its lack of response to tritium gas puffing, even when this raises the neutron emission by a large factor (e.g. the 2 MA/2T discharge number 42517) and its lack of response to very high neutron yields, as shown in Fig.6.

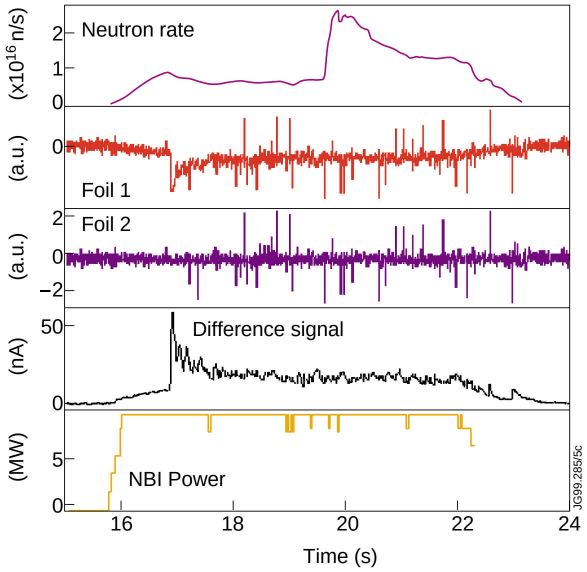

Fig. 5. Discharge 42517: signals processed as in the previous figure. At 19.6 s a puff of tritium is allowed to enter the vacuum vessel, when the neutron signal (predominantly due to d-t neutrons) rises sharply. Despite the low plasma current and toroidal field values of 2 MA, 2 T for which the alpha-particle detection efficiency should be reasonably high, there is no accompanying change in the signals recorded by the foils.

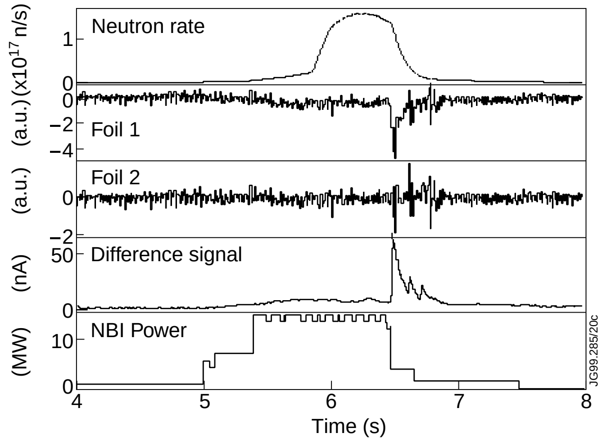

Fig. 6. The lack of an alpha-particle signal is shown very clearly for this reverse-shear discharge, number 42523 with Ip = 2.9 MA and B_T = 3.46 T. The event at 6.5 s is a giant ELM.

The accumulated evidence suggests the following interpretation of the first foil signal. The main ingredients are: (i) the fast ion population at large radii, just inside the separatrix, (ii) the density of neutrals just inside the plasma edge, (iii) the ion density in the scrape-off layer intersecting the detector entrance. Through charge-exchange processes, fast ions (mainly slowing-down beam-injected and ICRF-accelerated ions) close to the edge of the plasma become neutralized and a proportion will stream outwards towards the vessel walls. Of these, a small fraction will be ionized in the scrape-off layer. Those ions created within the volume of a flux tube linking the ionization position with the detector have a 50% chance of drifting towards the detector. Provided their Larmor radii are large enough (ion energy above about 10 keV), those ions with pitch angles falling in the appropriate range will have an appreciable probability of passing through the aperture in the detector and so reaching the first foil. Deuterons would need to have energies in excess of 500 keV in order to penetrate the first and so reach the second foil.

C. Qualitative interpretation

Because of the geometrical requirement that low energy ions confined within the flux tube leading to the detector need have only 6 mm minimum Larmor radii, the escaping deuterium neutrals of interest need not be very energetic, (e.g. > 10 keV at B_T = 3.4 T).

To estimate the fast ion density in a manner that can include ICRF heating, we assume one quarter of the measured total diamagnetic energy W (Joules, N.B. conversion factor 1.602×10^{-16}

J per keV) is distributed uniformly over the peripheral region of the plasma (considered here to be the outer 0.5 m thickness). Thus, the number of ions with average energy E_d per unit volume (60 m^3 of peripheral plasma) is, very approximately, $N_f = 2.6 \times 10^{13} \times W / E_d$ m^{-3} (or 1.5×10^{19} m^{-3} for $W = 10^7$ J and $E_d = 10$ keV). This figure should be representative for the outer plasma region. The effective ion loss rate is obtained from this particle density using the particle confinement time of $\tau_P \sim 0.5$ s that is typical of JET high performance discharges.

The thermal neutral density, N_0, at the plasma edge is obtained from the calibrated $D\alpha$ light emission ($D\alpha$, photons/s.sr.m^2) measured along a horizontal line-of sight. The conversion from photons to cold neutrals entering the plasma is given by the Johnson-Hinnov factor (taken to be ≈10, for typical edge plasma electron density and temperatures) and the typical life-time in the plasma of a bound electron before ionization is taken to be 3×10^{-6} s. Using 200 m^2 for the plasma surface area and 20 m^3 for its volume (10 cm thick edge region), gives $N_0 \sim 20 \times D\alpha$ m^{-3}. A typical value for $D\alpha$ is 10^{17} photons/s.sr.m^2.

We estimate the magnitude of the escaping fast neutral flux as follows:

$$\varphi \approx 20/200 \times (N_f / \tau_P) \times [1\text{-}\exp(- N_0 \times \sigma \times v \times \Delta t)] \times \exp(- n_{e\,edge} \times \sigma \times x) \qquad (1),$$

where x is the assumed effective thickness of plasma (0.10 m), σ is the charge-exchange cross-section (approximate value 10^{-19} m^2), Δt is the slowing down time for the fast ions at the plasma edge (~ 20 ms), $n_{e\,edge}$ is the edge plasma electron density (assuming $Z_{eff} \sim 1$) and v is the mean velocity of the fast ions. The first factor is the effective volume/surface ratio. The first exponential gives the probability of neutralization and the second that of not undergoing re-ionization before the neutral escapes from the edge. Simplifying, and with edge transparency set to unity since we have already assumed an effective thickness of 0.10 m, we find in m^{-2} s^{-1} units:

$$\varphi \approx 0.05 \times N_f / \tau_p \times N_0 \times \sigma \times v \times \Delta t \qquad (2).$$

The total loss power thus attributed to fast neutrals (usually, slowing down beam ions) is typically ~ 1 MW for JET discharges with applied beam powers of 10 to 20 MW, in approximate agreement with values obtained from the transport code TRANSP [8].

We assume the e-folding length for the ion density in the scrape-off layer is about 1.5 cm, so that at 10 cm from the separatrix the density would be nearly 10^{17} m^{-3} for density limit discharges if the exponential fall-off continued for 6 decay lengths. This value is comparable with the neutral gas pressure, P, as measured with Penning gauges near the vacuum pumps, which is typically ~ 10^{-5} mb. The gauges measure in mb, so $N_g = 1.34\times10^{22} \times P$ m^{-3}. Thus, the typical deuterium density is $N_g = 10^{17}$ m^{-3} at 600 K. The background gas pressure outside the plasma boundary is assumed to be less than the (fully ionized) plasma density at that point. The signal from the first foil is found to have a correlation coefficient with the Penning pressure of nearly zero, whereas that with the central electron density is significant. It is understood that the ion density in the scrape-off layer decreases exponentially for only a few decay lengths, and then flattens off. Accordingly, we take $N_g \approx n_e \times 10^{-2}$ m^{-3}, where n_e is the axial electron density.

The geometry of the detector and its neighbouring poloidal limiter is such that the detector collects charged fast ions from a flux tube of about 1 cm diameter by 1 metre long. The ionization probability for neutrals crossing this flux tube will be $\Pi_i = 10^{-23} \times N_g$. (Using a volume of 10^{-4} m^3). We have again invoked the charge-exchange cross-section σ.

Finally, we make some assumptions about the efficiency with which fast charged particles within the acceptance flux tube can enter the detector and reach the first foil, which is screened penetrated by an earthed plate penetrated by a number of small holes - giving an effective area of 3.7 cm^2. For this to be possible, the gyro-radius must exceed 6 mm and the pitch angle needs to be appropriate to the energy; for $\rho \sim 10$ mm, the relevant range of angles is, very approximately, from 45^o to 60^o . Recognizing the toroidal field dependence, we roughly estimate the collection efficiency of the detector as $\varepsilon \sim 3.4 / B_T \times 1\%$. The current detected by the first foil is:

$$I_{1st\ foil} = \varphi \times \Pi_i \times \varepsilon / (6 \times 10^9)\ \text{nA} \qquad (1)$$

where

$\varphi = 1 \times 10^{-16} \times N_f \times N_0$,
$N_f = 2.5 \times 10^{13} \times W / E_d$, with $E_d \sim 10$ keV,
$N_0 = 20 \times D\alpha$,
$\Pi_i = 10^{-23} \times N_g$,
$N_g = n_e \times 10^{-2}\ m^{-3}$,
$\varepsilon = 3.4/B_T \times 0.01$.

or $I_{1st\ foil} = 2.8 \times 10^{-38} \times n_e \times W \times D\alpha / B_T$ (nA units). The current-voltage relationship for the detector is 200 nA $\equiv$ 10 volts. The constant multiplier is only expected to be accurate to an order of magnitude but the dependence on the other quantities should be reliable. In practice, it is found that the above expression reproduces the time-dependence of the first foil signal very well, as shown in Figs. 7 to 12, which are presented in order of increasing toroidal field/plasma current.

Fig. 7 shows that the simple formula performs extremely well at low toroidal field and plasma current for deuterium beam-heated discharges. Figs. 8 and 9 illustrate the result that larger signals recorded when tritium beams, as opposed to deuterium beams, are employed for heating purposes, as expected from their respective Larmor radii. Fig. 10 shows that the formula over-predicts the signal for stronger toroidal fields, perhaps indicating that the Larmor radius constraint on particle selection is cutting into the energy distribution of the escaping neutrals, which is over-simplified by the simple inverse dependence on toroidal field strength. Fig. 11 shows that, even though the toroidal field and plasma current are close to 4 T and 4 MA, there is quite a strong measured signal provided tritium beam heating is employed.

Finally, as shown in Fig. 12, the temporal response of the predicted signal does not track that of the measured signal faithfully in the case of ICRF-only heating, although the magnitude is comparable with that for beam heating. Fig. 12 also indicates the necessity to subtract off a

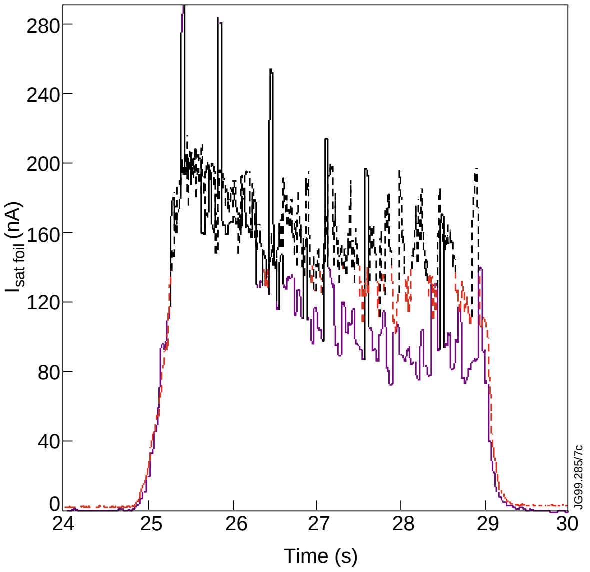

Fig. 7. Discharge 43135: equation 1 (solid line) with an adjustment factor of 1.7 reproduces the measured current (dashed line) for this 0.95 MA, 0.95 T, deuterium beam-heated discharge.

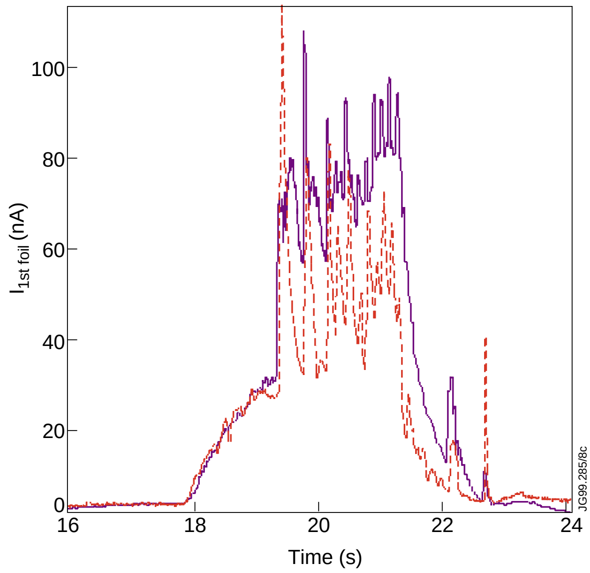

Fig. 8. Discharge 42794: equation 1 (solid line) with an adjustment factor of 0.5 reproduces the measured current (dashed line) quite closely for this 1.75 MA, 1.78 T , tritium beam-heated discharge.

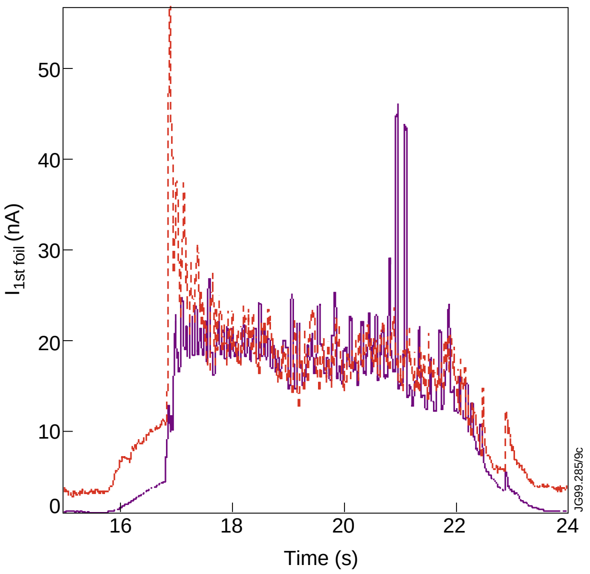

Fig. 9. Discharge 42517: equation 1 (solid line) under-estimates the measured current (dashed line). An adjustment factor of 6 is needed to obtain a fit for this 2 MA, 2 T , deuterium beam-heated discharge.

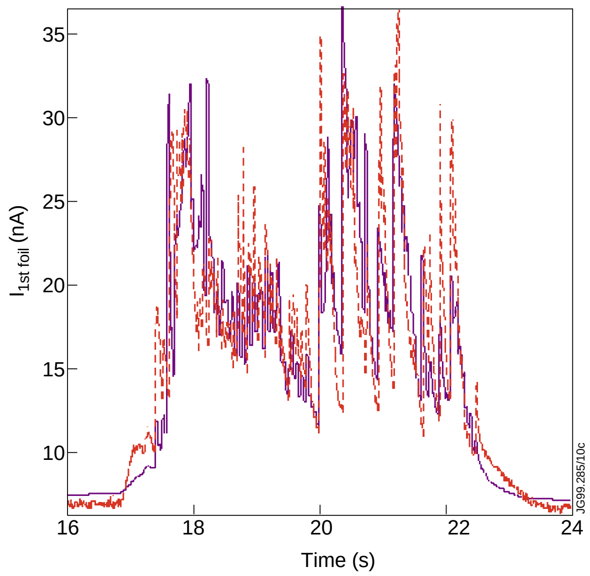

Fig. 10. Overlay of the recorded current (dashed line) and the prediction of equation 1 (solid line) scaled and given an off-set to obtain a good fit for deuterium beamed discharge number 43141, with Ip = 3 MA, B_T = 3 T. An adjustment factor of 6 is needed to obtain the fit. The time-dependence is dictated by the D_α signal.

large standing current drawn from the first foil. An analysis of all the discharges in the campaign studied, referred to below, showed that the presence of the standing current began to be observable at about midway through the campaign and the level thereafter increased linearly with discharge number. This is believed to have been due to the formation of a carbon deposit, within the detector head, that provided a leakage path to the potential of the screening rings.

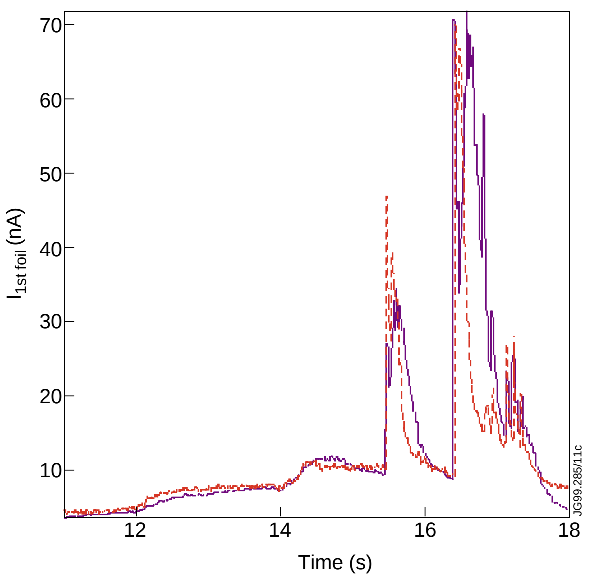

Fig 11. Discharge 42992: overlay of the recorded current (dashed line) and the prediction of equation 1 (solid line). The time-dependence is dictated by the D_α signal. An adjustment factor of 3 is needed to obtain the fit for this Ip = 3.8 MA, B_T = 3.9 T, tritium beam heated discharge.

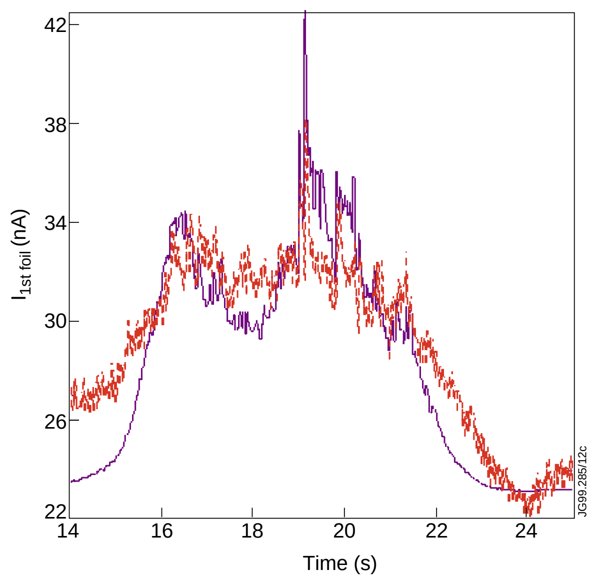

Fig. 12. Discharge 43550: 11 MW RF heated, 2.76 MA, 2.60 T. Only trace tritium presence. The detector signal has a constant current drain of 23 nA, which has been subtracted. To obtain the above fit, the equation 1 has been multiplied by 6 (as was the case for the comparable deuterium beam-heated case).

To predict the magnitude of the signal to better than order-of-magnitude accuracy would be a major task. However, the evident agreement between the calculation and the observations (particularly the time dependence) gives strong support for our interpretation. It is not surprising that a study of individual discharges shows that a considerable scatter exists between observed and predicted signal level absolute magnitudes. This is shown in Fig.13, which displays the results of a statistical study in which the measured signals from the first foil, averaged over 50 ms before and after the peak neutron emission during each discharge, are compared with the calculated values using the above simple formula. The study covered the DTE1 experiment. There is no correlation with neutron yield. 700 discharges are represented, comprising a mixture of ohmic, beam, ICRF and combined heating. The plasma current ranged from 0.75 to 4.45 MA and the toroidal field from 1.18 to 4.0 T. The scale factor has been adjusted slightly to improve the fit. The overall correlation can be improved by restricted data selection. The calculated results appear to cover at least two decades whereas the measured currents cover little more than one. This is at least partly due to not isolating hydrogen, deuterium and tritium beam fuelled discharges. Also, this form of plot gives undue weighting to the giant ELMs, which may obscure underlying trends.

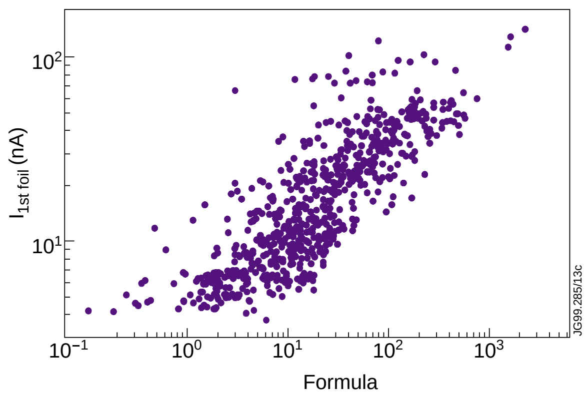

Fig. 13. Comparison of measured signals, averaged over 50 ms before and after the peak neutron emission during each discharge, with the calculated values using the formula (equ.1) (DTE1 data).

IV. RESULTS FROM THE MKIIGB DIVERTOR CAMPAIGN

A. Observations

Data from the thin foil Faraday collector were analyzed for all discharges in the campaign (range 44645-46435) subsequent to the installation of the MkIIGB divertor that took place after the DTE1 experiment. It became clear from the start that the character of the recorded signals had suffered a major change, the overall response being far weaker than hitherto and the predictive formula was no longer successful. To help elucidate matters, another statistical survey was carried out in a similar manner to that used for the DTE1 data

For this second campaign, the signals were normally very small but on occasion large signals were observed, when the first foil showed the higher signal (positive and sometimes saturating at 200 nA) while the second foils was negative and much lower (or zero). No obvious signals were found in the third and fourth foils.

Correlations between the first foil current ($I_{1st\ foil}$) and the other quantities in the database were sought, with none of them being particularly evident except for the presence of non-zero $I_{1st\ foil}$ when both ICRH and NBI were simultaneously applied. The results are shown in Figs. 14 to 16. In Fig.14 the 1st foil current signal is plotted as a function of NBI power, showing the existence of a cluster of discharges producing large signals. Fig. 15 shows the same plot with all ICRH-heated discharges removed; no discharges exhibiting significant signals were found. However, Fig. 16 shows that in a few cases a small signal is present during ICRH even though no NBI is applied. To summarize, ICRH appears to be necessary for a significant $I_{1st\ foil}$ to be observed, and the additional application of NBI is helpful. However, simultaneous application of both forms of heating does not guarantee a non-zero signal.

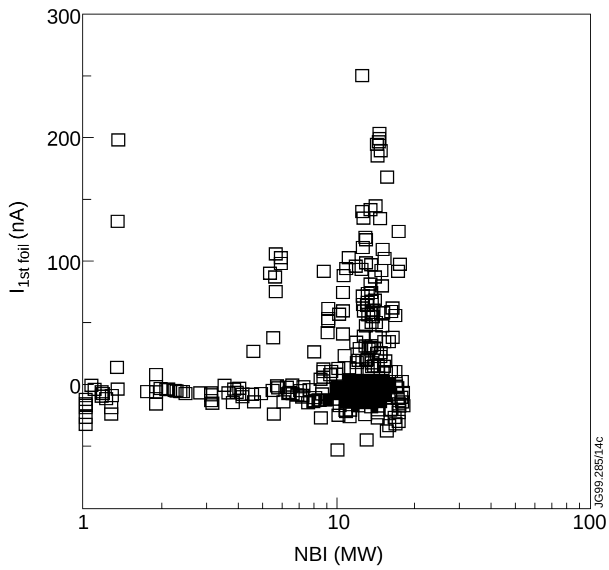

Fig. 14. Current from 1st foil vs NBI power (quantities are 100 ms averages centred at peak neutron emission for discharges) with ICRH power (MkIIGB data).

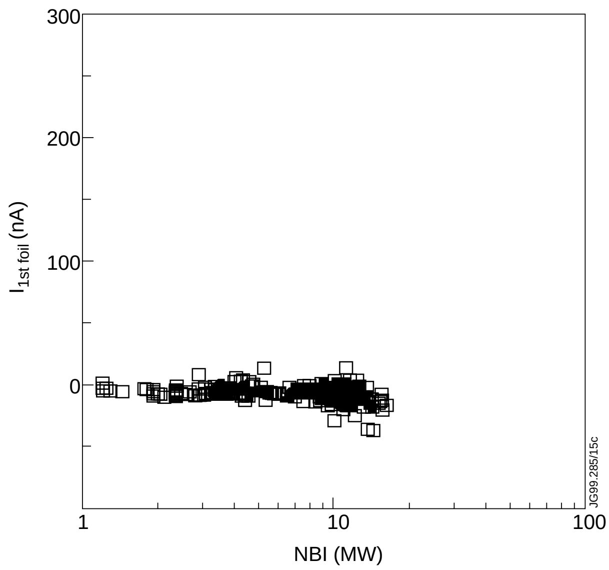

Fig. 15. Current from 1st foil vs neutral beam power at peak neutron emission for discharges without ICRH power (MkIIGB data).

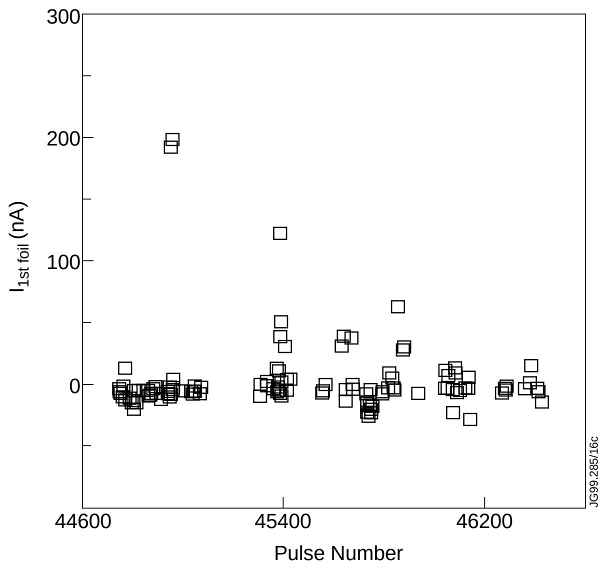

Fig. 16. Current from 1st foil vs shot number for discharges with ICRH power and no NBI power (MkIIGB data, early conditioning discharges are not included).

When the discharges with high $I_{1st\ foil}$ are selected from Fig. 14 ($I_{1st\ foil}$ > 25 nA and NBI > 4 MW) it is found that nearly all of them were part of the optimized shear experimental program. Some of these discharges terminated in a disruption (when the high $I_{1st\ foil}$ value was found at the moment of disruption) and others had krypton or argon gases injected. The signal from the first foil is usually found to commence its increase about 200 ms or more (see Fig. 17) after the application of ICRH power, suggesting that time is needed for the acceleration of light ions to detectably high energies. In some discharges the $I_{1st\ foil}$ signal appears to be correlated with an increase of the Penning gauge pressure (Figs. 17 and 18). Finally, the horizontal D_α signal sometimes shows a temporal correlation with $I_{1st\ foil}$: see Fig. 17, where the spikes in the D_α signal are quite well reproduced in the first foil signal (but which was almost always the case in the DTE1 campaign).

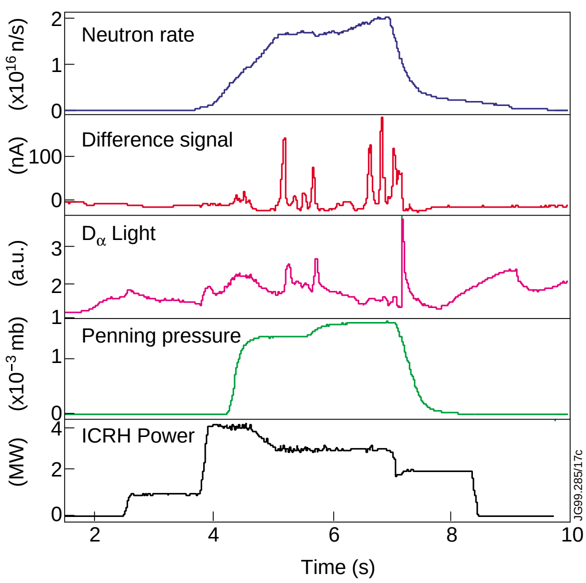

Fig. 17. Time traces of neutron emission, $I_{1st\ foil}$, horizontal D_α, Penning pressure and ICRH power in discharge 46123.

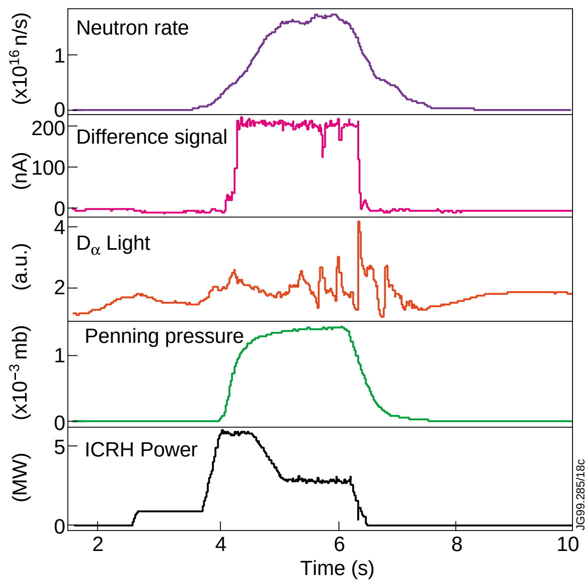

Fig. 18. Time traces of neutron emission, $I_{1st\ foil}$, horizontal D_α, Penning pressure and ICRH power in discharge 45888. Note the saturation in the $I_{1st\ foil}$ signal and the approximately same timing in the increase/ decrease of $I_{1st\ foil}$ and Penning pressure.

B. Discussion

The results from the MkIIGB campaign are different from those of the DTE1 campaign in so far as the correlation previously found, $I_{1st\ foil} \propto n_e \times W \times D_\alpha / B_T$, is lost and the connection between $I_{1st\ foil}$ and the D_α signal is much less clear than before. In order to explain these findings, we assume that plasma density in the scrape-off layer falls more rapidly with separation in the MKIIGB configuration than was the case for MkIIA, as appears probable from an inspection of the newer divertor boundary surface geometry. Presumably, during DTE1 the scrape-off layer density was sufficiently high that rather low energy particles (>10 keV, with Larmor radii of > 5 mm) could easily enter the Faraday collector whereas with the MkIIGB divertor the scrape-off layer density fall-off is faster and, to compensate for this, the particles must have larger Larmor radii if they are to reach the collector (i.e. energies >> 10 keV). Moreover, because the probability of recording a large signal is now so greatly reduced, the sensitivity to local conditions (e.g.: an increase of the local gas pressure can also increase the ionization and therefore $I_{1st\ foil}$) is likely to be much greater. We note that the energy of the detected particles cannot be much above 500 keV otherwise the signal would have been observed not only in the 1st foil but in other foils as well since there is no need for these ions (unlike alpha-particles) to enter the detector at angles far from the normal to the plane containing the collectors.

Therefore, the most probable explanation of the signal in the 1st foil during the MkIIGB divertor campaign is that, for detection, the ions must have energies above that associated with beam injection, so that RF acceleration is necessary. Energetic RF-accelerated particles are most likely to follow orbits leading to the plasma edge when optimized shear discharges are being produced, since the axial safety factors are quite large (up to 3) and fast particle confinement is correspondingly poor. In addition, the optimized shear discharges have low densities and high temperatures in the peripheral region (outside r/a = 0.5), permitting the fast particles to survive longer than usual in the plasma and enhancing their loss through charge-exchange processes.

V. CONCLUSION

Although the foil charge collectors were installed with the intention of measuring a current of lost alpha-particles, such currents were not convincingly observed. This is explained by the large distance between the detector and the plasma boundary, which prevented measurable currents of lost alpha-particles from entering the detector except possibly under conditions of broad alpha-particle source profiles, high fusion powers and low toroidal fields. The detector was not commissioned at the time when the only discharges answering this description were run. On the positive side, the diagnostic proved immune to high fluxes of 14-MeV neutrons and it was possible to detect currents as low as 1 nA without suffering electrical interference effects. It is reasonable to hope that a more robust, more compact, design of detector head with larger sensitive area could be positioned closer to the plasma so that the goal of detecting alpha-particle currents could be achieved during future D-T experiments.

The strong signals that were recorded on the first foil of the detector were not anticipated, although their explanation now seems obvious. Order-of-magnitude calculations of the loss of energetic neutrals from the plasma surface and their re-ionization in the low pressure gas in the vicinity of the detector leads to the prediction of a signal level that is very much in accord with observations for the DTE1 campaign. This interpretation also applies to the data obtained after the installation of the new MkIIGB divertor, although the assumed sharper scrape-off layer limits particle collection to higher energies so that the presence of ICRH power becomes a necessary condition for the detection of a non-zero first foil current, with the poor particle confinement associated with optimized shear discharges being most advantageous.

The design of any lost alpha-particle system to be constructed in the future using current sensing will have to address this neutralization/re-ionization problem and a thin first foil to filter out low energy charged particles will probably be needed. Such a detector should be positioned much closer to the separatrix than was the case in the present experiment, although this would presumably give rise to an even larger current due to escaping neutrals. Finally, we note that the mechanism described here indicates that energetic fast particles can become implanted in surfaces that do not have a direct view of the plasma (e.g *behind* the poloidal limiters).

REFERENCES

[1] H.W.Herrmann, S.J.Zweben, D.S.Darrow, et al., "Deuterium-tritium results of TFTR's alpha collector", Nuclear Fusion **37** (1997) 293.

[2] D.S.Darrow, S.J.Zweben, H.W.Herrmann, "Alpha-particle loss diagnostics in TFTR and tokamak reactors", Fusion Engineering and Design **34-35** (1997) 53.

[3] M.J.Loughlin, F.E.Cecil, M.Hone, O.N.Jarvis, S.Medley, A.L.Roquemore, G.J.Sadler, P. van Belle and G.Whitfield, "Evaluation of ITER-compatible thin foil Faraday collector as a lost alpha-particle diagnostic for high yield d-t tokamak plasmas", Rev. Sci. Instrum. **68** (1997) 36.

[4] O.N.Jarvis, S.W.Conroy, M.Hone, G.J.Sadler, P. van Belle, "15-MeV proton emission from ICRF-heated plasmas", Controlled Fusion and Plasma Physics, Vol. 18B, Part I, pp. 270-273, (Proc 21st Europ Conf, Montpellier, 1994.

[5] The JET Team (presented by A.Gibson), "D-T plasmas in the Joint European Torus (JET): Behaviour and implications", JET-P(97)58. To be published in the Journal of Plasma Physics (1998).

[6] F.E.Cecil, B.Roy, S.Kern, A.Nowak, Y.Takimoto, O.N.Jarvis, P. van Belle, G.J.Sadler, M.Hone, M.Loughlin, D.Darrow, S.S.Medley, L.Roquemore, C.Barbour, "Development and operation of a thin foil faraday collector as a lost ion diagnostic for high yield d-t tokamak fusion plasmas", High Temperature Plasma Diagnostics Meeting, American Physical Society, June 6-12, 1998, Princeton, U.S.A.

[7] N.Hill, "A review of ELMs in divertor tokamaks", Journal of Nuclear Materials **241-243** (1997) 182.

[8] R.V.Budny et al., Nuclear Fusion **3**2 (1992) 429.

[9] F.E. Cecil et al., Rev. Sci. Instrum., **70**(1) (1999), 1149.